Fig. S1 Example analysis in a single spatial region. **a** Location of the spatial domain shown in the example. **b** The rectangular target region of the analysis, showing the cases of $l = 0.2°$ (cyan) and $l = 0.4°$ (magenta). **c** Time series of M and cumulative number of earthquakes of $M \geq 2.0$ in the target region. **d** FMD. Symbols and solid lines indicate non-integration and integration of larger magnitude earthquakes, respectively. **e**–**g** Time series of estimated b-, η-, and D-values, respectively. In **c**–**g**, symbol colors correspond to the rectangular regions shown in **b**.

Fig. S2 Probability density distributions of index values for the FMD expected from the GR law. One million M-series data were generated for each of the four different true b-values using random numbers. Each index value was calculated by extracting N values in order. **a** PDDs of observed b-values normalized by the true b-value. This distribution is independent of the true b-values and depends only on N. **b** PDDs of η-values. This index value is independent of b and depends only on N without normalization.

Fig. S3 The expected relationship between D, normalized by N, and $\min T_{N/4}$ in the case of a stationary Poisson distribution. The period of the tidal response is assumed to be constant at 12 h, and the mean occurrence interval and initial phase are randomly chosen to generate the occurrence time series following a stationary Poisson distribution. D and $\min T_{N/4}$ were estimated 100,000 times each for $N = 50$ and $N = 100$. The vertical dashed line marks 21,600 s (6 h).

Fig. S4 An example of a FMD with which it is difficult to estimate M_c. The inset shows the corresponding $M - t$ plot. A large earthquake and its early aftershocks are included at the end of the analysis period, resulting in an unusually small b-value (0.34 with $M_{th} = 1.95$) due to the effect of reduced detectability. When the analysis period is set uniformly, as in this study, it is necessary to devise a method to discriminate such a partial decrease in detectability during the analysis period.

Fig. S5 Same as Figure 4, but using the EMR method to estimate M_c.

Fig. S6 Same as Figure 14, but for the relationship between b^+ and $\min T_{N/4}$. The relatively high b^+-value for small values of $\min T_{N/4}$ (< 300 s) in **a** is probably a result of the decrease in detectability.

Figure S1

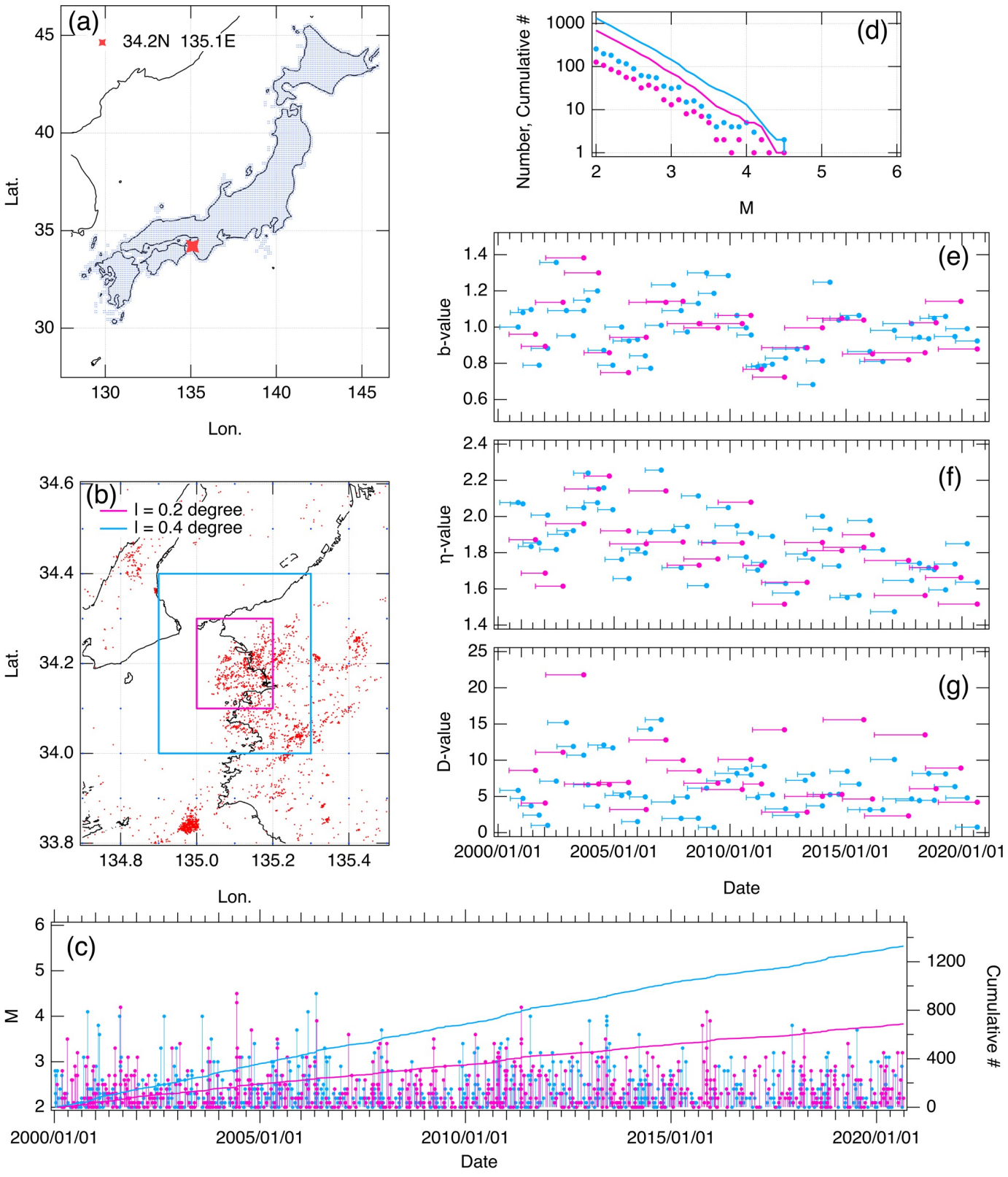
(a)
34.2N 135.1E
Lat.
Lon.
(b)
l = 0.2 degree
l = 0.4 degree
Lat.
Lon.
(c)
M
Cumulative #
Date
(d)
Number, Cumulative #
M
(e)
b-value
(f)
η-value
(g)
D-value
Date

Figure S2

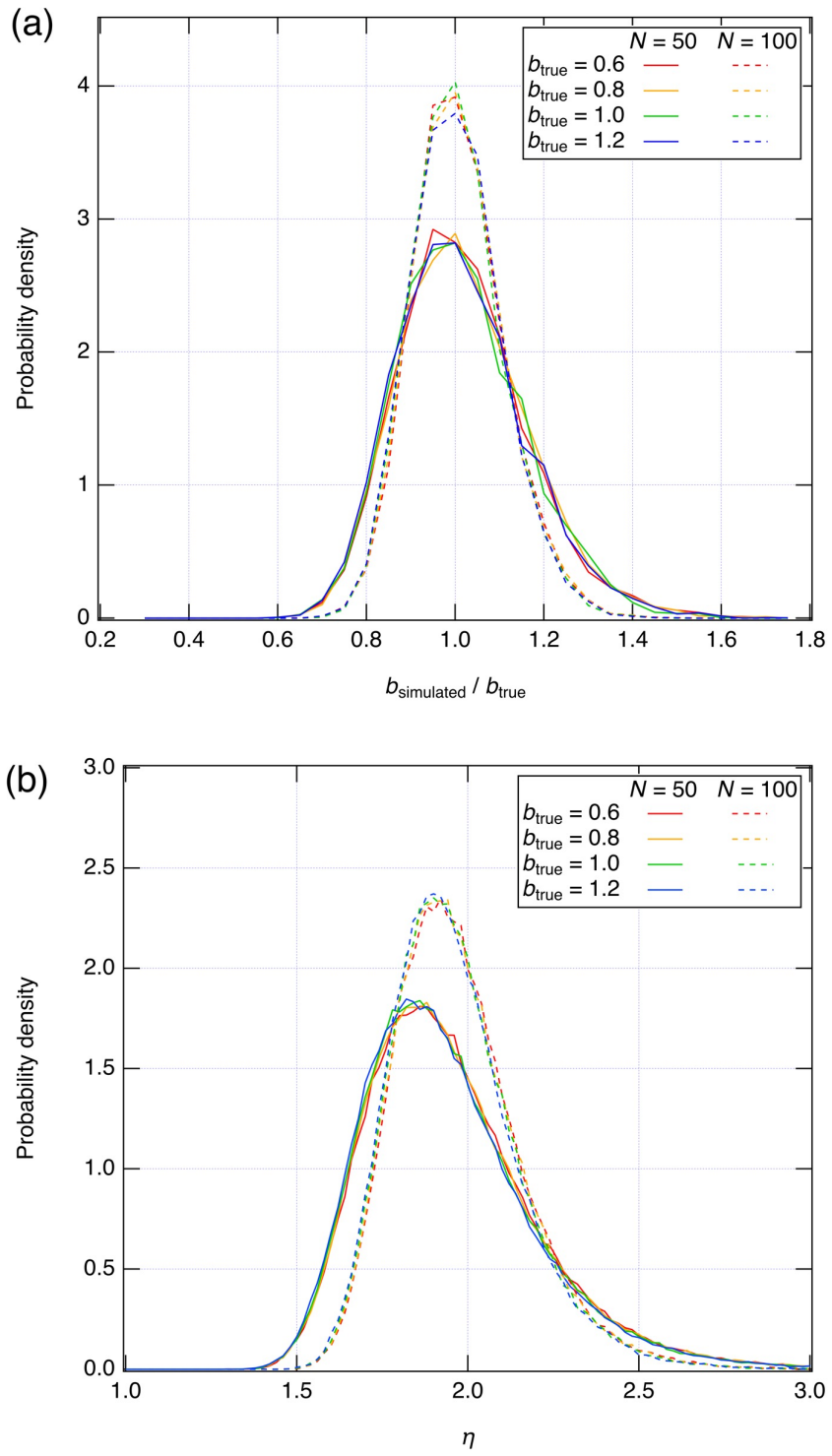
(a)
N = 50
N = 100
b_true = 0.6
b_true = 0.8
b_true = 1.0
b_true = 1.2
Probability density
b_simulated / b_true
(b)
N = 50
N = 100
b_true = 0.6
b_true = 0.8
b_true = 1.0
b_true = 1.2
Probability density
η

Figure S3

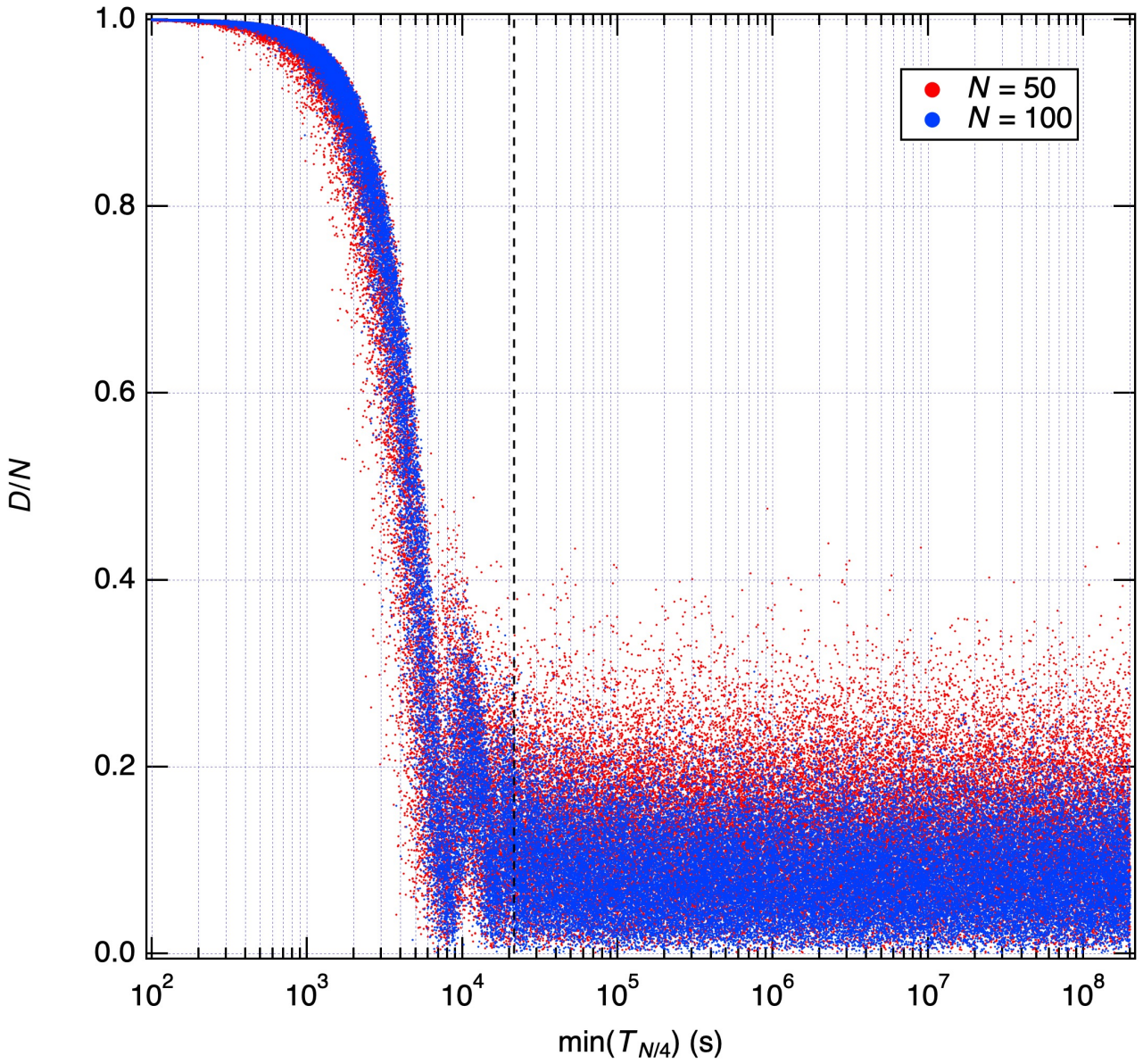

Figure S4

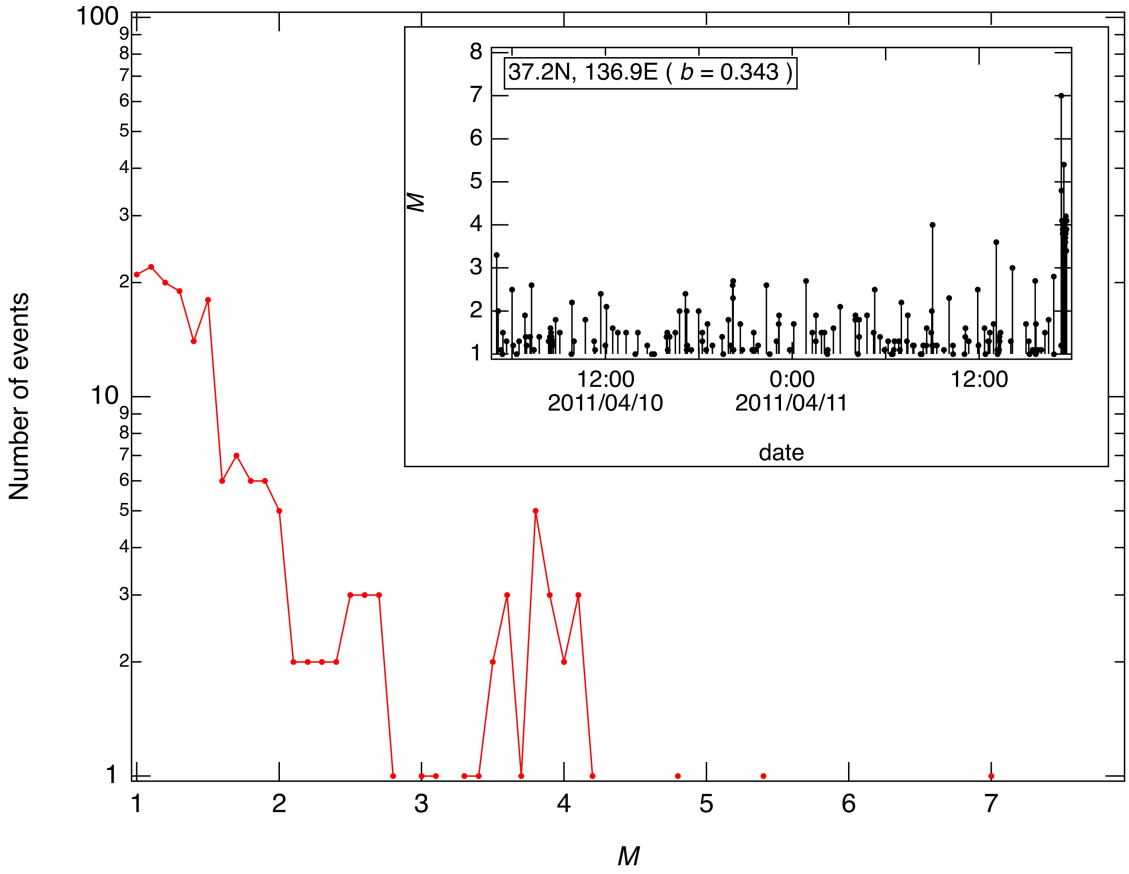
Number of events
M
37.2N, 136.9E (b = 0.343)
M
12:00
2011/04/10
0:00
2011/04/11
12:00
date

Figure S5

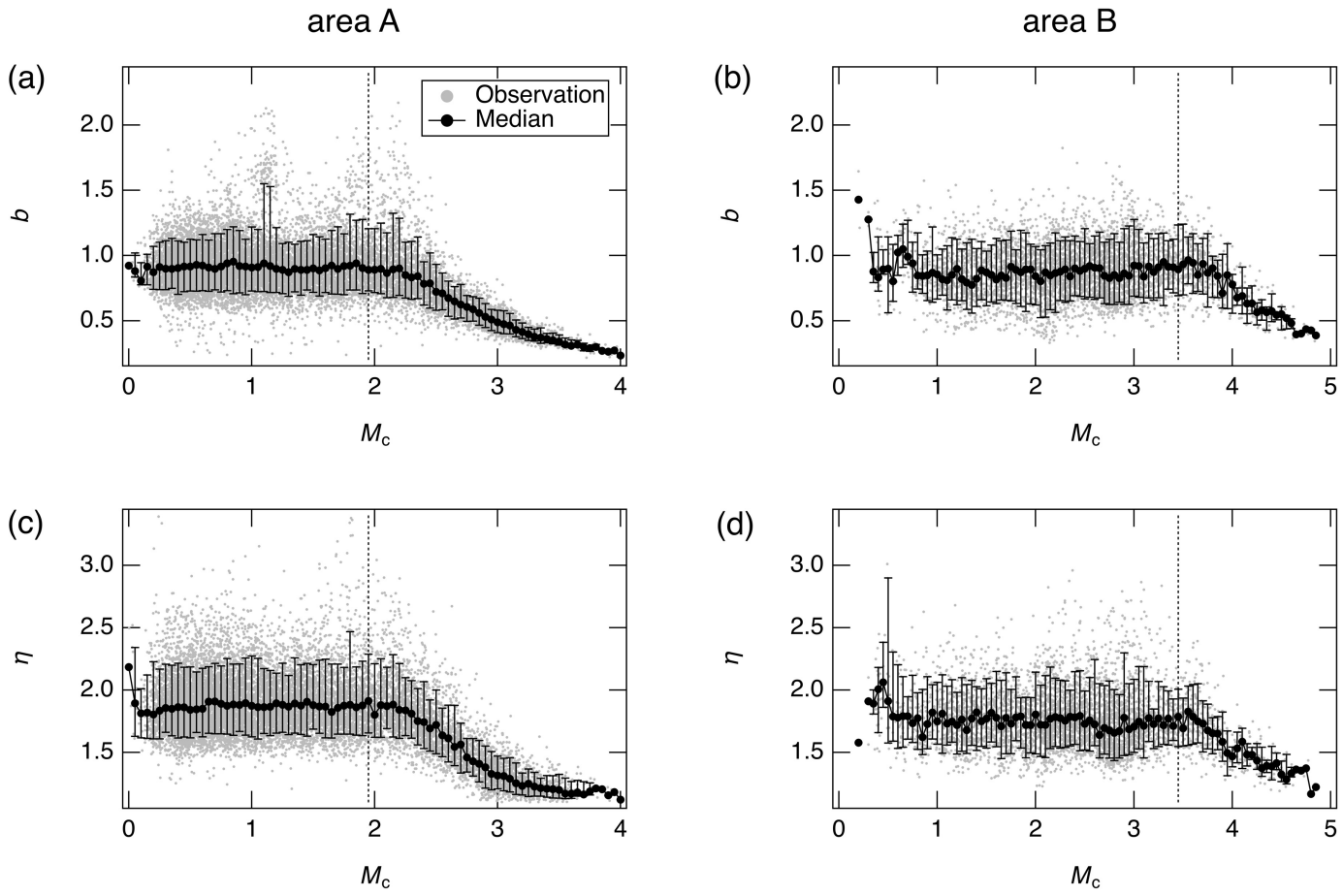
area A
area B
(a)
(b)
(c)
(d)
Observation
Median
b
η
M_c
0
1
2
3
4
5
0.5
1.0
1.5
2.0
2.5
3.0

Figure S6

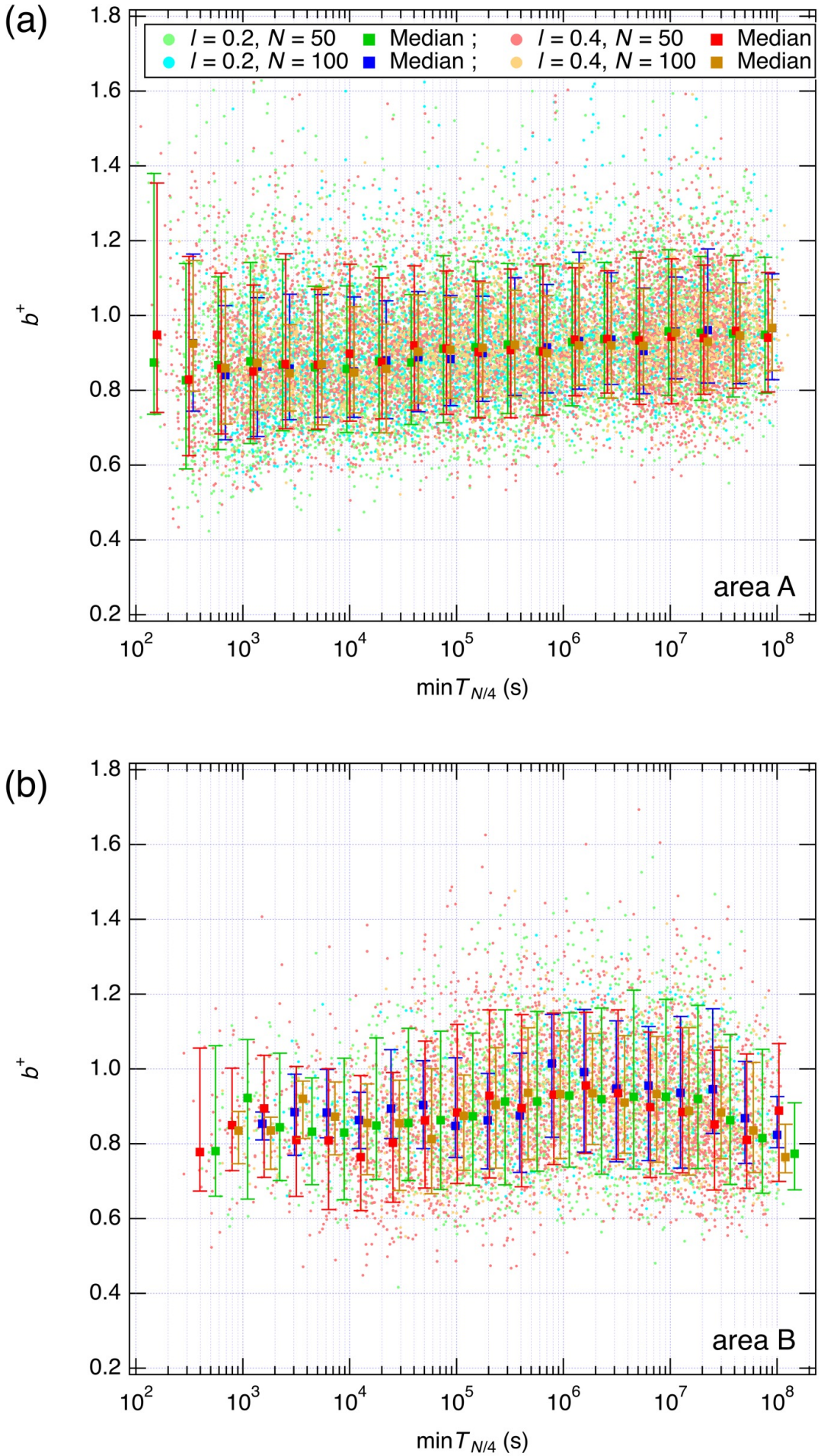
(a)
l = 0.2, N = 50
Median ;
l = 0.4, N = 50
Median
l = 0.2, N = 100
Median ;
l = 0.4, N = 100
Median
b+
area A
min T N/4 (s)
(b)
b+
area B
min T N/4 (s)